Application of fractional Gaussian Fractal-Based Stochastic Seismic Inversion to F3-Netherland dataset

Srishti Singh, Sreeja Kalyankar, Ajay Malkoti, and Nimisha Vedanti
CSIR-National Geophysical Research Institute, Hyderabad-500007, India

SUMMARY

Estimating the seismic impedance from the band-limited seismic data has proven to be a difficult task, especially due to the absence of low frequencies. This situation can be mitigated using the information obtained from well logs which can be used as a constraint. This prior information can be incorporated in various forms and for the stochastic technique, the statistics followed by the logs can be used. In case of fractal based inversion, we used the fractal characteristics of the well log to produce fractal-based models. The inversion module minimizes a suitable objective function using very fast simulated annealing (VFSA) algorithm. We demonstrated the effectiveness of this inversion technique on a 2D line extracted from F3-Netherlands dataset.

INTRODUCTION

Seismic inversion is an integral tool for carrying out the reservoir characterization. It helps in determining the elastic properties of a given reservoir (e.g. acoustic impedance, elastic moduli) by inverting the seismic data, and thereby determining lithology, porosity, fluid saturation, etc. Conventionally, the results obtained by inverting seismic data only (e.g. relative inversion) are devoid of low and high frequencies due to the band limitation of the seismic data (Russell, 1988). The geophysical borehole data is sampled at a very fine scale and therefore it contains all scales of information. This prior information can be used to increase the resolution of the inverted data. Generally, there are two types of techniques for inversion– deterministic and stochastic. Deterministic inversion techniques are based on the principle of minimization of the differences between the seismic data and the synthetic/modeled data (Özdemir, 2009; Francis, 2006; Russell, 1988). The inversion outputs in such cases are relatively smooth or blocky estimates of impedance. Such inversion is suitable for relatively thick layered reservoirs where lateral thickness changes slowly with minimal spatial impedance variation (Francis, 2006).

Stochastic inversion techniques, on the other hand, generate a large number of possible impedance solutions, aka realizations, that may give a good match to observed seismic data (Haas and Dubrule, 1994; Bosch et al., 2010; Liu and Grana, 2018; Srivastava and Sen, 2010). An advantage of stochastic algorithms is their ability to incorporate various geophysical information with seismic to enhance the inversion result. Usually, well logs are used in addition to the seismic data to improve the vertical resolution of the inversion outputs. Combining well-log data as apriori information with seismic data also enhances the low-frequency content of the model parameters. Therefore, generating initial models containing a realistic frequency band is very important. Random Gaussian priors have been extensively used as the initial model in standard stochastic inversions. However, Gaussian priors contain a white spectrum, therefore the high- and low-frequency components of the initial model are not constrained by the inversion algorithms as these frequency bands are absent in seismic data.

In this work, we have used the fractal-based stochastic inversion technique (Srivastava and Sen, 2010). It first, generates initial models based upon the fractal characteristics of the geophysical borehole data, which also serves as the initial guess for the inversion algorithm. The acoustic impedance is estimated using a global optimization technique called very fast simulated annealing (VFSA) which generates different solution iteratively and selects the impedance model based on heat-bath algorithm (Sen et al., 1995). The inverted impedance model are used to generate synthetic seismograms through forward convolution modelling. These inverted synthetic Data are then compared to input seismic data to obtain a good match. The entire process is performed iteratively, till the solutions converge.

THEORY

The basic premise while inverting the seismic data is that seismic data can be described using the convolution model. It means that the seismic data can be represented as the convolution of the source wavelet and the reflectivity of the earth. Mathematically it can be written as the following.

$$x(t) = s(t) * r(t) + n(t), \tag{1}$$

Here, $x(t)$ is the observed seismic trace, $s(t)$ is the source wavelet, $r(t)$ is the earth's true reflectivity, and $n(t)$ is the noise. The convolution model assumes the data to be noise-free and from any other effect (e.g. non-linearity, dispersion of source, etc.). If we assume a stacked layer of earth with N-number of layers then for the k^{th}-layer reflectivity can be determined as follows.

$$r_k = \frac{I_{k+1} - I_k}{I_{k+1} - I_k}, \tag{2}$$

where, I_k is the acoustic impedance of the layer, which is equal to the product of density (ρ_k) and velocity (v_k) of the given layer, i.e. $I_k = \rho_k v_k$.

Seismic Inversion is an estimation of acoustic impedance from seismic data, which is a non-linear inverse problem (eq. (2)). To solve this nonlinear problem of acoustic impedance estimation, a global optimization technique, very fast simulated annealing (VFSA) is used. This inversion module requires an initial model as starting solution. To build the initial model, we generate trace-by-trace 1D fractal time-series realization of acoustic impedance model by using the fractional Gaussian process (Caccia et al., 1997). The fractional Gaussian noise for 1D time series (σ) consists of normally distributed random variables with zero mean and an auto-covariance function given by

$$R(\tau) = 0.5\sigma^2(|\tau+1|^{2H} - 2|\tau|^{2H} + |\tau-1|^{2H}), \qquad (3)$$

where, τ is the time separation of random variables, and H is the Hurst coefficient. The fractional Gaussian noise are generated by fractional Gaussian process so that both the mean and the auto-covariance function for the generated time series follow the mean and auto-covariance of the input time series (well log), respectively. These generated time series are used as an input to VFSA inversion module as a starting solution.

VFSA method is based on the simulated annealing (SA) optimization description given by Kirkpatrick et al. (1983). In SA, a function of a large number of parameters is minimized through a Monte Carlo approach. The mathematical framework of annealing uses the analogy between model parameters and heating of a solid material. Heating a solid beyond its melting point and cooling slowly to form crystals is referred to as state of minimum energy. This state is analogous to the minimum error in an optimization problem. Stochastically, each configuration of solid particles is known as a state. As the temperature decreases, the solid is brought into thermal equilibrium at each temperature, where the likelihood of a particle occupying a state i with energy E_i (analogous to the error function in optimization) is determined by the following Gibb's or Boltzmann probability density function (Sen et al., 1995):

$$P(E_i) = \frac{\exp(-\frac{E_i}{KT})}{\sum\limits_{j\in S} \exp\frac{E_j}{KT}} = \frac{1}{Z(T)}\exp(-\frac{E_i}{KT}) \qquad (4)$$

where S denotes all possible configurations, K is Boltzmann's constant, T is temperature and the partition function Z(t) is given as follows:

$$Z(T) = \sum_{j\in S} \exp\frac{E_j}{KT} \qquad (5)$$

After thermal equilibrium is achieved, the temperature is gradually decreased. As the temperature approaches zero, the probability of the system occupying the state with the minimum energy increases significantly. In VFSA, each model parameter is allowed to have different finite range of variations. The perturbations in model parameters in NM dimensional space are given as follows:

$$m_i^{k+1} = k_i^k + y_i(m_i^{max} - m_i^{min}) \qquad (6)$$

$$y_i = sgn(u_i - 0.5)T_i\left[\left(1+\frac{1}{T_i}\right)^{|u_i-1|} - 1\right] \qquad (7)$$

where m_i^k is the model parameter for the k^{th} iteration, u is the random number between [0,1] and T_i is the i^{th} parameter's temperature in k^{th} iteration. The cooling scheme adapted in VFSA module for each T_i of k^{th} iteration is given by:

$$T_i(k) = T_0\exp(-c_i k^{1/NM}), \qquad (8)$$

where, T_0 is the global temperature and c_i is the decay parameter.

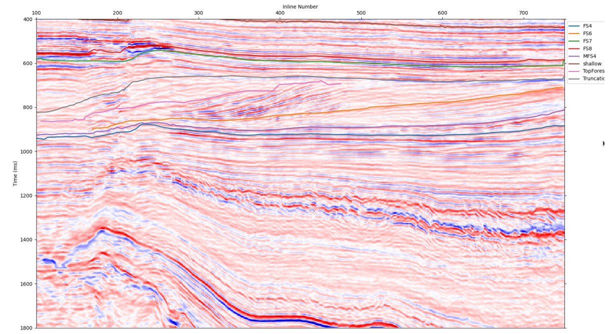

Figure 1: A 2D seismic data (poststack) extracted from 3D F3-Netherlands data (crossline:1008). All available horizons are labeled on the right, however, the data between FS8 and FS4 only is used for inversion.

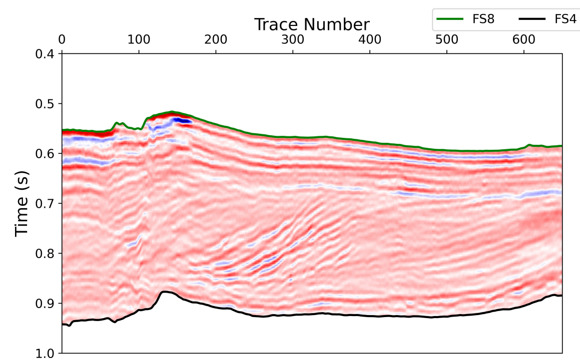

Figure 2: Original seismic data used as input for inversion. Here, only two horizons (FS8 and FS4) were considered. The seismic section was extracted from 3D F3 Netherlands offshore data.

RESULTS

We inverted a 2D line data (crossline:1008) extracted from F3 Netherlands Offshore data (Figure 1). The inversion was performed on this seismic data only between two horizons, FS4 and FS8, depicted by red and blue colors in Figure 1, respectively. The region of interest is shown in the Figure 2. The well F03-4 lies at inline 441, which contains density, sonic, Gamma Ray and porosity logs. After the pre-conditioning of well log data, we computed acoustic impedance and reflectivity logs using the density and sonic logs. Both horizons, FS8 and FS4 lie at depths of ~568 m and ~946.5 m in the well logs. Therefore, we used the well logs between these two horizons for building initial models. Before that, the time-to-depth conversion was performed using the sonic log and check-shot data. Then, both seismic and well-logs data were interpolated and sampled equally to maintain consistency.

To run inversion for the entire geometry, we interpolated acoustic impedance logs from well F03-4 for the entire 2D line, after applying well-seismic tie. The low frequency initial model (Figure 3) was obtained by applying a low pass filter to the interpolated logs.

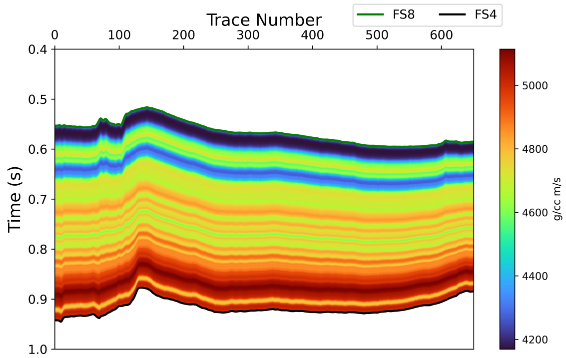

Figure 3: Low frequency acoustic impedance model obtained by first interpolating the well log impedance data (at cross-line: 1008) between given horizons and then spreading it across the model in between the given horizons.

It is important to ensure the given logs follow the fractal behavior other the inversion may fail. Therefore, we checked for the fractal behavior of these well logs by performing R/S analysis and the slope of these plots gave the Hurst coefficient (H). Figure 4 shows R/S analysis of impedance trace 340, where blue dotted line in Figure 4 represents a slope of 0.5 i.e. $H = 0.5$, while red dotted line is for the case when $H = 1.0$. The R/S analysis of acoustic impedance of trace 340 shows that the best fitting line is much closer to $H = 1.0$ (nearly parallel to $H = 1.0$ line) and yields a Hurst coefficient of 0.949, thus displaying a strong fractal behavior.

As we have the statistical characteristics of the log data (i.e. mean, variance and Hurst coefficient) we can generate the fractional Gaussian noise for each trace through fractional Gaussian process algorithm. Considering these fractal-based time series realizations as starting solutions, we ran VFSA module to invert for the impedance, so that inverted synthetics match the seismic data. The final impedance model obtained after running several iterations of stochastic inversion is shown in Figure 5. Inverted impedance model shows significant variations. The shallower regions ($< 0.6s$) have lower impedance beds of $\sim$ 3500 g/cc*m/s, while the impedance near FS4 horizon is found to be $>$ 5500 g/cc*m/s. There are non-horizontal alternate bands of high and low impedances in between $0.6s - 0.9s$ for traces from 150 to 350.

The validity of the inverted results can be assessed by simply comparing the synthetics generated using this inverted model and the inverted model. The synthetic seismograms are shown in Figure 6 which is in very much agreement of the original data (Figure 2). The difference between observed seismic data and inverted synthetic seismograms is displayed in Figure 7.

CONCLUSIONS

We have inverted a 2D section (poststack) from F3 Netherlands dataset, between two horizons, namely FS8 and FS4. Borehole data from well F3-04 at inline 441 was used to generate apriori models for inversion. Before generating initial models, we

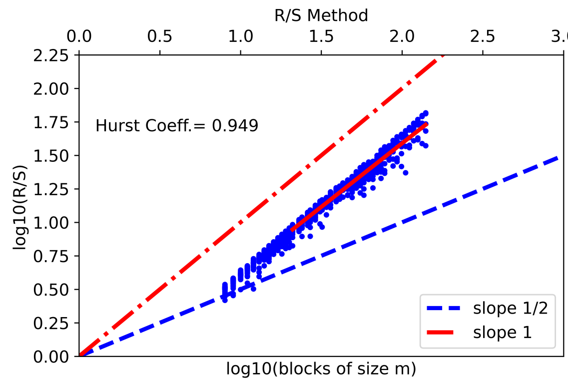

Figure 4: Plot of R/S analysis of interpolated impedance for trace 340. Hurst coefficient (H = 0.949) given by slope shows the fractional Gaussian noise characteristic of the well log.

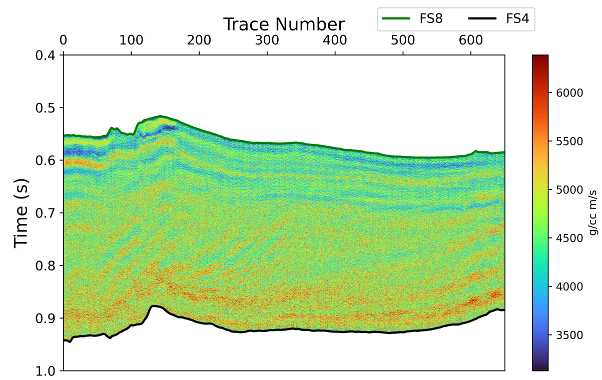

Figure 5: The inverted impedance model obtained after running VFSA inversion module.

conducted a check on whether borehole data satisfied the statistical characteristics required for fractal-based stochastic inversion. The Hurst coefficient was found to be greater than 0.5, thus showing that well logs exhibited fractal behaviour. Using the Hurst coefficient, mean and standard deviation of acoustic impedance, low frequency initial models were generated that acted as initial solutions to VFSA algorithm. After several iterations, we obtained best impedance model for the entire line. The final impedance model showed significant variations in impedances along the seismic data variations (Figure 1) as opposed to the initial impedance model in Figure 3. The final impedance model corresponds to the inverted synthetics which best match the observed data in between both horizons. The difference in both inverted synthetic and observed seismic data can be further used for uncertainty analysis. Fractal-based stochastic inversion allows the incorporation of constraints like the Hurst coefficient and covariance computed using the Hurst coefficient, which enforces convergence. It is computationally cheap and also advantageous over deterministic inversions, as it can detect and delineate thin spatial reservoir units.

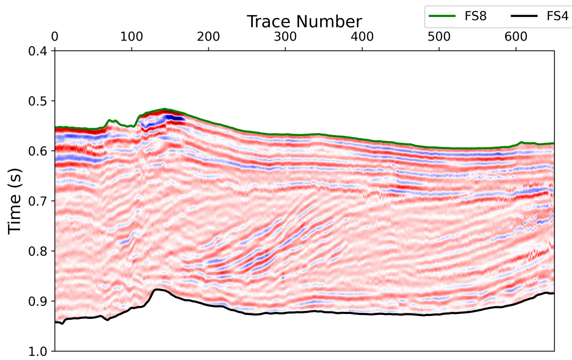

Figure 6: Synthetic seismograms for entire 2D line, corresponding to the best-fit model derived by stochastic inversion algorithm.

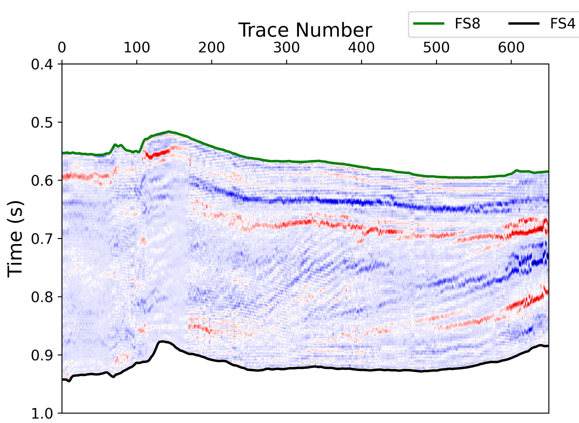

Figure 7: The difference between both, original and synthetic seismograms, which may be used to quantify uncertainty in our inversion.

ACKNOWLEDGMENT

Authors thank Director, CSIR-NGRI for his permission to publish this work. We are also very thankful to Dr. M. K Sen, and Dr. R. P. Srivastava for their valuable inputs. All results were generated using the inhouse developed seismic inversion package under the project MLP-6402-FTT-001-28.

REFERENCES

Bosch, M., T. Mukerji, and E. F. Gonzalez, 2010, Seismic inversion for reservoir properties combining statistical rock physics and geostatistics: A review: Geophysics, **75**, 75A165–75A176.

Caccia, D. C., D. Percival, M. J. Cannon, G. Raymond, and J. B. Bassingthwaighte, 1997, Analyzing exact fractal time series: evaluating dispersional analysis and rescaled range methods: Physica A: Statistical Mechanics and its Applications, **246**, 609–632.

Francis, A., 2006, Understanding stochastic inversion: Part 1: First Break, **24**.

Haas, A., and O. Dubrule, 1994, Geostatistical inversion-a sequential method of stochastic reservoir modelling constrained by seismic data: First break, **12**.

Kirkpatrick, S., C. D. Gelatt Jr, and M. P. Vecchi, 1983, Optimization by simulated annealing: science, **220**, 671–680.

Liu, M., and D. Grana, 2018, Stochastic nonlinear inversion of seismic data for the estimation of petroelastic properties using the ensemble smoother and data reparameterization: Geophysics, **83**, M25–M39.

Özdemir, H., 2009, Unbiased deterministic seismic inversion: more seismic, less model: first break, **27**.

Russell, B. H., 1988, Introduction to seismic inversion methods: SEG Books.

Sen, M. K., A. Datta-Gupta, P. Stoffa, L. Lake, and G. Pope, 1995, Stochastic reservoir modeling using simulated annealing and genetic algorithms: SPE Formation Evaluation, **10**, 49–55.

Srivastava, R. P., and M. K. Sen, 2010, Stochastic inversion of prestack seismic data using fractal-based initial models: Geophysics, **75**, R47–R59.